

ORIGINAL ARTICLE

Cellular iron depletion enhances behavioral rhythm by limiting brain *Per1* expression in mice

Qiong Wu^{1,2} | Qiuyang Ren¹ | Xin Wang¹ | Huiyuan Bai¹ | Dandan Tian¹ |
Guofen Gao¹ | Fudi Wang³ | Peng Yu¹ | Yan-Zhong Chang¹ 

¹Laboratory of Molecular Iron Metabolism, Key Laboratory of Molecular and Cellular Biology of Ministry of Education, Hebei Key Laboratory of Animal Physiology, Biochemistry and Molecular Biology, Hebei Collaborative Innovation Center for Eco-Environment, Hebei Research Center of the Basic Discipline of Cell Biology, College of Life Sciences, Hebei Normal University, Shijiazhuang, China

²Hebei Key Laboratory of Chinese Medicine Research on Cardio-Cerebrovascular Disease, College of Basic Medicine, Hebei University of Chinese Medicine, Shijiazhuang, Hebei Province, China

³School of Public Health, Zhejiang University School of Medicine, Hangzhou, Zhejiang, China

Correspondence

Yan-Zhong Chang and Peng Yu,
Laboratory of Molecular Iron Metabolism,
Key Laboratory of Molecular and Cellular
Biology of Ministry of Education, Hebei
Key Laboratory of Animal Physiology,
Biochemistry and Molecular Biology,
Hebei Collaborative Innovation Center for
Eco-Environment, Hebei Research Center
of the Basic Discipline of Cell Biology,
College of Life Sciences, Hebei Normal
University, Shijiazhuang 050024, China.
Email: yzchang@hebtu.edu.cn,
chang7676@163.com and
yupeng0311@163.com

Funding information

Natural Science Foundation of Hebei
Province, Grant/Award Number:
C2023423008 and H2019423032; Basic
research program for young teachers of
Hebei University of Chinese Medicine,
Grant/Award Number: YQ2018007; Hebei
Research Center of the Basic Discipline
of Cell Biology, Grant/Award Number:
C2023205049; Science Research Project
of Hebei Education Department, Grant/
Award Number: BJK2023095; National
Natural Science Foundation of China,
Grant/Award Number: 32070962

Abstract

Aims: Disturbances in the circadian rhythm are positively correlated with the processes of aging and related neurodegenerative diseases, which are also associated with brain iron accumulation. However, the role of brain iron in regulating the biological rhythm is poorly understood. In this study, we investigated the impact of brain iron levels on the spontaneous locomotor activity of mice with altered brain iron levels and further explored the potential mechanisms governing these effects *in vitro*.

Results: Our results revealed that conditional knockout of *ferroportin 1* (*Fpn1*) in cerebral microvascular endothelial cells led to brain iron deficiency, subsequently resulting in enhanced locomotor activity and increased expression of clock genes, including the circadian locomotor output cycles kaput protein (*Clock*) and brain and muscle ARNT-like 1 (*Bmal1*). Concomitantly, the levels of period circadian regulator 1 (*PER1*), which functions as a transcriptional repressor in regulating biological rhythm, were decreased. Conversely, the elevated brain iron levels in APP/PS1 mice inhibited autonomous rhythmic activity. Additionally, our findings demonstrate a significant decrease in serum melatonin levels in *Fpn1^{cdh5}*-CKO mice compared with the *Fpn1^{flox/flox}* group. In contrast, APP/PS1 mice with brain iron deposition exhibited higher serum melatonin levels than the WT group. Furthermore, in the human glioma cell line, U251, we observed reduced *PER1* expression upon iron limitation by deferoxamine (DFO; iron chelator) or endogenous overexpression of *FPN1*. When U251 cells were made iron-replete by supplementation with ferric ammonium citrate (FAC) or increased iron import through transferrin receptor 1 (*TfR1*) overexpression, *PER1* protein levels were increased. Additionally, we obtained similar results to U251 cells in mouse cerebellar

The first three authors contributed equally to this work.

This is an open access article under the terms of the [Creative Commons Attribution](https://creativecommons.org/licenses/by/4.0/) License, which permits use, distribution and reproduction in any medium, provided the original work is properly cited.

© 2024 The Authors. *CNS Neuroscience & Therapeutics* published by John Wiley & Sons Ltd.

astrocytes (MA-c), where we collected cells at different time points to investigate the rhythmic expression of core clock genes and the impact of DFO or FAC treatment on PER1 protein levels.

Conclusion: These findings collectively suggest that altered iron levels influence the circadian rhythm by regulating PER1 expression and thereby modulating the molecular circadian clock. In conclusion, our study identifies the regulation of brain iron levels as a potential new target for treating age-related disruptions in the circadian rhythm.

KEYWORDS

aging, circadian rhythm, clock genes, iron, Per1

1 | INTRODUCTION

The circadian clock, which is mainly controlled by the suprachiasmatic nucleus (SCN) of the hypothalamus, coordinates the internal functions of the organism within 24-h, self-perpetuating oscillations.¹ The circadian system possesses crucial roles in most physiological processes, including sleep alertness and various areas of cognitive performance. Circadian misalignment is widespread in the elderly, who often exhibit declined sleep quality. Furthermore, there is an accumulation of misalignment with age since the circadian rhythm cannot be completely resorted by recovery sleep.^{2,3} Additionally, aging-related neurodegenerative diseases, which are usually accompanied by cognitive impairment, can also disrupt rhythmic oscillations.⁴ Importantly, several studies have shown that perturbation of regular biological rhythms, linked to the pathologies of diseases such as Alzheimer's disease (AD), ischemic stroke, other mental disorders, and cancer,⁴⁻⁸ results in numerous physiological disorders in organismal homeostasis, ultimately affecting quality of life.⁹

Iron is an essential participant and regulator of various fundamental physiological activities.¹⁰ Several studies have demonstrated that aging is accompanied by elevated cellular iron deposition. Abnormal iron accumulation and the consequential induction of redox stress have been widely reported to participate in the pathogenesis of aging-related neurodegenerative diseases.¹¹⁻¹³ At the same time, disruptions in circadian rhythms have also been increasingly recognized as symptoms of aging and age-associated neurodegenerative disorders, including AD.^{14,15} Clinical and animal model studies have further revealed the presence of progressive circadian dysfunction throughout the course of these diseases.^{16,17} However, few studies have investigated the effects of iron or brain iron levels on circadian rhythm maintenance. Liu et al. reported that iron accumulation with age altered the metabolic pattern and expression of circadian clock genes through decreased histone methylation in the mouse liver.¹⁸ Additionally, iron-induced redox toxicity may also lead to a disturbance in the biological circadian clock. A recent review by T. Ishii et al. discusses how circadian rhythm-induced improvements in the expression of an important antioxidant pathway, brain-derived neurotrophic factor (BDNF)-Nrf2 in astrocytes, can strengthen astrocyte-neuron interactions and protect dopaminergic neurons from

iron-mediated cell death (ferroptosis) and redox toxicity in rodent brains.¹⁹ Thus, it is important to understand whether alterations in iron status can alter biological rhythms and affect the expression of circadian clock genes.

In the present study, we investigated the influence of altered brain iron levels on locomotor activity and circadian rhythms in 10-month-old mice. Mice with conditional knockout of the cellular iron exporter, FPN1, in microvascular endothelial cells (*Fpn1^{Cdh5}-cKO*) were used in this study since they display low brain iron levels.²⁰ We also used APP/PS1 double-transgenic mice that are reported to exhibit brain iron accumulation with age.²¹ The *Fpn1^{Cdh5}-cKO* mice exhibited increased locomotor activity, while the APP/PS1 mice displayed inhibited rhythmic activities. Our initial results suggest that mice with altered brain iron levels possess altered behavioral rhythms. We proceeded to investigate the regulation of the transcriptional/translational feedback loop (TTFL) comprising the clock genes and their corresponding proteins.^{22,23} The TTFL is responsible for maintaining the oscillation system and synchronizing the cycle with the environment. In TTFL regulation, the core clock gene, PER1, acts as a transcriptional repressor, while CLOCK functions as an enhancer that can promote rhythmic activities.^{24,25} We found that *Fpn1^{Cdh5}-cKO* mice with declined brain iron levels exhibit decreased expression of Per1, with elevated CLOCK levels. These results imply that alterations in brain iron levels can indeed alter circadian clock gene expression and lead to modified TTFL regulation. Finally, we investigated the potential molecular mechanisms involved in the effects of iron on clock gene regulation in U251 cells. We conclude that iron can modulate the activity of the PER1-CLOCK-BMAL1 regulatory pathway. We propose rhythmic regulation of brain iron levels as a novel target to improve age-related disruption of the circadian rhythm.

2 | MATERIALS AND METHODS

2.1 | Animals

Ten-month-old wild-type (WT) mice, APP/PS1 transgenic mice, *Fpn1^{flox/flox}* mice, and *Fpn1^{Cdh5}-cKO* mice were used in this study. The APP/PS1 double-transgenic mice and WT control mice are

in the C57BL/6J background and were purchased from Beijing Zhongke Zesheng Technology Co., Ltd (Beijing, China). The APP/PS1 mice were crossed with WT mice, and the genotypes of the offspring were previously determined.²¹ The VE-Cadherin-Cre (Cdh5-Cre) transgenic mice on a C57BL/6 genetic background used in the study were a generous gift from Dr. Xiao Yang of the Beijing Institute of Life Omics, and were characterized in previous study.²⁶ In the present study, we generated *Fpn1*^{Cdh5}-cKO mice by mating Cdh5-Cre mice with *Fpn1*^{flox/flox} mice on a C57BL/6 background. The genotypes of the Cdh5-Cre and *Fpn1*^{flox/flox} mice were described previously.²⁰ All the mice were bred and maintained in a specific pathogen-free (SPF) animal facility under a 12h light and 12h dark cycle. Mice were allowed free access to water and food and were randomly assigned to experimental groups. All procedures were carried out in accordance with the National Institutes of Health Guide for the Care and Use of Laboratory Animals and approved by the Animals Ethics Committee of Hebei Normal University, China.

2.2 | Experimental design and measurement of rodent locomotor activity

Male mice were used in all experiments. The locomotor activities of 10-month-old mice were analyzed ($n=3-4$ per group). The recordings of locomotor activity spanned 8 consecutive days, including 6 days of normal light/dark cycles (LD, 12:12, with lights on at 8:00 a.m. = zeitgeber time (ZT) 00) and 2 days of dark/dark (DD) cycles. The animals were acclimated to the experimental conditions for at least 5 days prior to the experiments. Individual mice were housed in cages equipped with infrared movement detectors connected to an automated recording system (the Mouse Wheel Running Activity Monitoring System, ZS-Labmaze IV, Beijing Zhongshi Dichuang Technology Development Co., Ltd., Beijing, China). Spontaneous locomotor activity was continuously recorded throughout the entire experiment and analyzed using Trigger Master software (v4.1.0, Beijing Zhongshi Dichuang Technology Development Co., Ltd., Beijing, China).

2.3 | Cell culture and treatment

U251 cells and MA-c cells were maintained in DMEM with high glucose, supplemented with 10% fetal calf serum and 100 U/mL penicillin/streptomycin at 37°C and 5% CO₂. Overexpression and knockdown of *Per1* were achieved by transfecting pcDNA3.1-*Per1* plasmid and si-*Per1*, respectively. The full-length coding sequence (CDS) of *Per1* (NM_002616.3) was inserted into the vector. The shRNAs (shRNA1, 2, and 3) for *Per1* were designed and synthesized by Youbio Technology, China. For cellular transfection, U251 cells were seeded in six-well plates, and grown to 90% confluence before transfection. The cells were transiently transfected with

pcDNA3.1 (empty vector, EV, 2500 ng), *PER1* overexpression plasmid (pcDNA3.1-*PER1*, 2500 ng), or the shRNAs (shRNA1, 2, and 3) for *PER1* (2500 ng). Transient transfection was performed using Lipofectamine 3000 (#MAN0009872, Invitrogen) according to the manufacturer's instructions.

The duration of treatment of U251 and MA-c cells with DFO or FAC was 24 h. To investigate the impact of collecting cells at different time points on the expression of circadian clock proteins, we used two time points. In the first approach, DFO or FAC was added to the cells at 10:00 p.m. on the first day. After 24 h (the following day at 10:00 p.m.), DFO or FAC was removed, and dexamethasone was added to the culture medium for 2 h (until midnight, 12:00 p.m.). On the morning of the third day at 8:00 a.m., the cells were harvested and immediately processed for subsequent studies. In the second dosing approach, the drug administration was the same as the first method, but the initial addition of DFO or FAC was performed at 10:00 a.m. Consequently, the collection and processing of cells were performed at 8:00 p.m. on the second day.

For the other cells in this study, we applied dexamethasone at 10:00 p.m. on the first day to induce synchronization, removed dexamethasone after 2 h, and collected the cells at 8:00 a.m. on the second day. These treatments help ensure that the cells are in a synchronized state, which is beneficial for studying the impact of circadian clock protein expression.

2.4 | Preparation of human glioma U251 cells overexpressing FPN1 or TfR1

The full-length CDS of the target gene, *FPN1* (NM_014585.6) or *TFR1* (NM_001128148.3), was inserted into a lentivirus vector that confers Puro resistance and is regulated by the TetOne operator (pLVX-TetOne-puro-SLC40A1 and pLVX-TetOne-puro-TFRC). The virus was generated by transfection into the HEK293T cells. The modified lentivirus was then prepared to infect U251 cells. After drug resistance screening, clones were selected and expanded for culture to establish U251 cell lines stably overexpressing *FPN1* (U251-FPN1) or *TfR1* (U251-TfR1). The U251-FPN1 and U251-TfR1 cells required induction with 100 nM doxycycline for 2 h to overexpress the respective proteins prior to additional treatments.

2.5 | MTT assay

The MTT assay was used to evaluate cell viability. After treatment with a gradient of FAC (#F5879, Sigma) or DFO (#D9533, Sigma), the culture medium was discarded, MTT (0.5 mg/mL, #M8180, Solarbio) was added, and the cells were incubated at 37°C in a 5% CO₂ incubator for 4 h. DMSO (150 μ L, #D8371, Solarbio) was then added to dissolve the formazan, and the absorbance at 575 nm was measured using a microplate reader (Synergy H4, Bio-Tek, USA).

2.6 | Enzyme-linked immunosorbent assay (ELISA)

Mouse serum levels of melatonin were measured using a commercial ELISA kit (E-EL-M0788c, Elabscience, Wuhan, China). All experimental steps were performed at room temperature and in duplicate. Samples were quantified by spectrophotometry at 450 nm.

2.7 | Immunohistochemistry (IHC) and double immunofluorescence (double-IF)

We used 15- μ m-thick, frozen brain slices containing the regions selected for investigation. The brain slices were washed three times in 0.01 M cold PBS and then incubated in 3% H₂O₂ for 10 min to quench endogenous peroxidase activity. Antigen retrieval was carried out in microwave oven in 0.01 M citric acid solution (pH 6) for 15 min. After washing with PBS, the sections were blocked in goat serum for 70 min at room temperature. Primary antibodies, including Ferritin-H (FtH, 1:400, #ab183781, Abcam), Ferritin-L (Ft-L, 1:200, #ab109373, Abcam), Per1 (1:100, #abs118499, Absin), or Clock (1:70, #5157s, Cell Signaling Technology), were added at 4°C overnight. For IHC staining, the sections were then incubated with biotin-labeled goat anti-rabbit serum for 1 h at 37°C after washing with PBS. Next, the brain slides were treated with an avidin-biotinylated horseradish peroxidase complex for 1 h at 37°C and stained using a DAB kit, followed by dehydration with an alcohol gradient, treatment with xylene, and sealing in adhesive resin. Images of the brain sections were acquired using an Axio Imager Z2 (Zeiss) attached to a tissue cytometer Tissue FAXS (TissueGnostics, Vienna, Austria). For double IF detection, after washing with PBS, the corresponding secondary antibodies, including DyLight 488 (1:200, #A23210, Abbkine) and DyLight 549 (1:200, #23320, Abbkine), were added at 37°C for 1 h, after which the sections were stained with DAPI (1:1000, #62248, Thermo Fisher). For double-IF experiments, the brain sections were scanned using an Olympus FV3000 confocal laser scanning microscope. The images were analyzed using imageJ software (National Institutes of Health).

2.8 | RNA isolation and quantitative real-time PCR (qRT-PCR) analysis

The total RNA from U251 cells or MA-c cells was extracted using TRIzol reagent, following the manufacturer's instructions. Total RNA (1 μ g) was reverse transcribed using MMLV reverse transcriptase with oligo-dT primers according to the manufacturer's instructions (#639574, Takara Bio, China). SYBR Green PCR Master Mix (#CW0659, CoWin Biosciences, China) was used for PCR amplification. The cycle time (Ct) values for the genes of interest were normalized to those of β -actin mRNA. The data were analyzed using the $\Delta\Delta$ Ct method. The primer sequences used for amplification were as follows:

BMAL1: forward-GGATGTGACCGAGGGAAGAT;
reverse- CGTCGTGCTCCAGAACAATAAT

PER1: forward- AACGGGATGTGTTTCGGGGTGC;
reverse- AGGACCTCCTCTGATTCCGGCAG

CLOCK: forward- GGGTTGGTGAAGAAGATGA;
reverse- AGCATTGTGAAGAAGATGA

CRY1: forward- CACTGGTTCGAAAGGGACTC;
reverse- CTGAAGCAAAAATCGCCACCT

ACTB: forward-AAGGGACTTCCTGTAACAATGCA;
reverse-CTGGAACGGTGAAGGTGACA.

2.9 | Western blot analysis

We previously described a method for protein extraction from various mouse brain regions (cortex and hippocampus).²⁷ For cellular proteins, we directly added RIPA buffer containing 1% NP40 and protease inhibitor cocktail tablets into the cell suspension to lyse the cells. After centrifugation, the supernatant was collected and the total protein concentration was measured using a BCA protein quantification kit (#20201ES76, Yeasen Biotechnology, Shanghai, China). About 20–40 μ g protein lysate was resolved by SDS-PAGE. The protein was then transferred to a nitrocellulose membrane, which was blocked in 5% nonfat milk dissolved in TBS-T for 1.5 h at room temperature. The desired primary antibodies FtL (1:5000, Abcam), FtH (1:5000, Abcam), FPN1 (1:10,000, #MTP11-S, ADI), Tfr1 (1:10,000, #13-6890, Abcam), PER1 (1:10,000, Absin, abs118499), Per2 (1:20,000, #67513-1-1 g, Proteintech Group), CLOCK (1:3000, Cell Signaling Technology), BMAL1 (1:8000, #14020S, Cell Signaling Technology), p-GSK3 β (1:5000, #9336, Cell Signaling Technology), or GSK-3 α/β (1:5000, #sc-7219, Santa Cruz) were then added at 4°C overnight. The membrane was washed with TBS-T, and then incubated with anti-rabbit or anti-mouse IgG secondary antibodies conjugated with horseradish peroxidase for 90 min at room temperature. After washing again with TBS-T, immunoreactive proteins were detected using the super ECL detection reagent kit (#36208ES60, Yeasen Biotechnology, Shanghai, China) and visualized using a chemiluminescence imager (Fujifilm Las-4000, Fujifilm, Japan). The relative band intensities of the proteins were quantified using imageJ software and are presented as the ratio of each to β -actin.

2.10 | Statistical analysis

The data are expressed as the mean \pm standard error of mean (SEM), as specifically indicated in the figure legends. The datasets were tested for normality distribution using the Shapiro–Wilk test using SPSS 21.0 software; those that passed the normality test were advanced to statistical analysis. The data were analyzed using a two-tailed Student's *t*-test for independent datasets and as specifically described in the figure legends. The data were analyzed using Prism v9.0 (GraphPad Software). *p* values <0.05 were considered statistically significant, while *p* values <0.01 were

considered remarkably significant. Data from this study are available from the corresponding authors, Yan-Zhong Chang and Peng Yu, upon reasonable request.

3 | RESULTS

3.1 | Altered brain iron levels results in shifts in locomotor activity rhythm

FPN1 is the only protein known to export cellular iron in mammals.²⁸ Conditional knockout of FPN1 in cerebral microvascular endothelial cells (*Fpn1^{Cdh5}-cKO*) inhibits the transport of peripheral iron into the brain through the blood–brain barrier (BBB), leading to brain iron deficiency.²⁰ FtH and FtL are cellular iron storage proteins that are usually used as indicators of uncommitted iron levels.²⁰ In the present study, we first examined the distribution and expression of FtH and FtL, in the SCN, cortex, and hippocampus of 10-month-old *Fpn1^{flox/flox}* and *Fpn1^{Cdh5}-cKO* mice. The *Fpn1^{Cdh5}-cKO* mice exhibited lower FtH and FtL levels in these brain regions compared to the controls, which is consistent with decreased iron, as we previously described in these mice (Figure 1A–E).²⁰

We next assessed the locomotor rhythms in the *Fpn1^{Cdh5}-cKO* mice. The results show that *Fpn1^{Cdh5}-cKO* mice had significantly increased locomotor activity compared to the *Fpn1^{flox/flox}* mice (Figure 1F–H). Several studies have demonstrated atypical brain iron accumulation in aged APP/PS1 mice.^{21,29} In contrast to the *Fpn1^{Cdh5}-cKO* mice, the APP/PS1 transgenic mice showed inhibited rhythmic activities compared to the WT mice which may be related to the elevated brain iron levels in these mice (Figure 1I–K).

Melatonin plays a crucial role in mammalian circadian rhythms, exhibiting diverse secretion levels during the light/dark phases of a day. Additionally, this neurohormone serves as a potent antioxidant.^{30,31} In our study, we conducted an ELISA assay using a mouse melatonin ELISA kit to measure serum melatonin levels. Our findings revealed a significant decrease in melatonin levels in *Fpn1^{Cdh5}-cKO* mice compared to the *Fpn1^{flox/flox}* control group. Conversely, in APP/PS1 mice with brain iron deposition, we observed greater serum melatonin levels than in the WT group (Figure 1L,M). These results demonstrate contrasting changes in serum melatonin levels in these two transgenic mice groups, which aligns with the hormone's role in circadian rhythm regulation. Moreover, our study suggests a potential link between brain iron status and circulating melatonin levels. Thus far, our results imply that lower brain iron levels in aging mice may promote locomotor activity and interfere with circadian rhythms.

3.2 | Brain iron deficiency leads to variation in the molecular circadian clock in *Fpn1^{Cdh5}-cKO* mice

The circadian rhythm is produced and regulated by the so-called “clock” genes. In the feedback loop composed by clock genes

and their encoded proteins, the BMAL1/CLOCK complex acts as a transcriptional activator of the genes encoding the repressor proteins, PER1 and PER2.^{32,33} In the present study, we examined the expression of PER1, CLOCK, and BMAL1 to investigate whether the decreased brain iron in *Fpn1^{Cdh5}-cKO* mice could impact the levels of these proteins. Immunostaining results revealed that there was an apparent decrease in PER1 and increased expression of CLOCK in the SCN and cortex of *Fpn1^{Cdh5}-cKO* mice (Figure 2A–E). Aligned with these results, western blot assays using cortical and hippocampal samples also revealed elevated CLOCK and diminished PER1 protein in cortex (Figure 2F,G). We did not see significant changes in PER1 and CLOCK expression in the hippocampus (Figure 2H,I). Collectively, our data suggest that alterations in brain iron levels can cause disturbances in circadian rhythms through the regulation of the TTFL composed by core clock genes.

3.3 | Exogenous cellular iron can regulate the expression of PER1, BMAL1, and CLOCK in U251 cells

In subsequent experiments, we examined the molecular mechanisms of cellular iron regulation of clock genes in vitro using the human glioma cell line, U251. First, we assessed the endogenous, rhythmic expression of *PER1*, *BMAL1*, *CLOCK*, and cryptochrome 1 (*CRY1*) in U251 cells (Figure S1). We observed the anticipated, rhythmic transcription of these genes in vitro, which aligns with their rhythms in vivo conducted in *Fpn1^{Cdh5}-cKO* mice. We then treated the U251 cells with different concentrations of the iron chelator, DFO, to deplete the cells of iron. Alternatively, we added ferric ammonium citrate (FAC) to the cells to generate an iron overload status. Based on cell viability, we selected 50 μM and 100 μM as the final concentrations of DFO and FAC, respectively (Figure S2).

After subjecting U251 cells to a 24 h treatment with 50 μM DFO, we selected two specific time points, 8:00 a.m. and 8:00 p.m., to explore the impact of cellular iron alterations on the protein expression of core clock genes. Figure 3 presents the results obtained from U251 cells collected at 8:00 a.m., while Figure S3 shows the protein levels of clock genes in U251 cells collected at 8:00 p.m.

In Figure 3, we first examined the protein levels of PER1, CLOCK, and BMAL1. Since BMAL1 can also be down-regulated by the p-GSK3β/GSK3β pathway,^{34,35} we evaluated the phosphorylation of GSK3β. Our results show diminished levels of FtH and FtL protein, indicating an iron starvation status in the DFO-treated cells. Additionally, PER1 protein levels were significantly decreased, while CLOCK levels exhibited an apparent increase, which is consistent with its down-regulation via PER1.³³ The western blot results also show markedly greater levels of phosphorylated GSK3β; however, we did not observe significant alterations in BMAL1 expression (Figure 3A–F). The latter is probably because of the bi-directional regulation of BMAL1 by PER1 and the p-GSK3β/GSK3β pathway. Our results preliminarily demonstrate that cellular iron status influences the expression of the circadian clock genes.

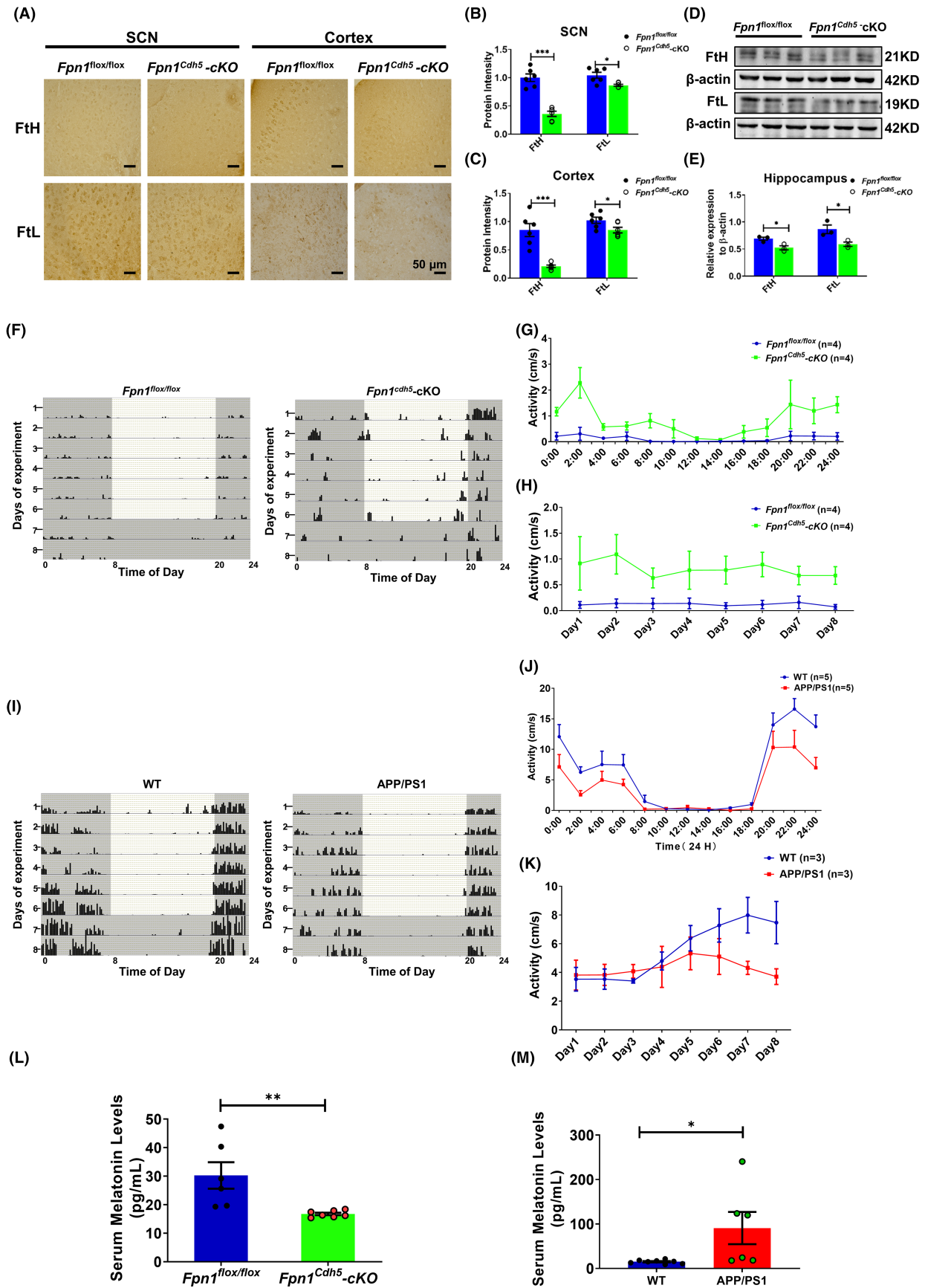


FIGURE 1 Altered expression of FtH and FtL in *Fpn1^{Cdh5}-cKO* mice and the locomotor activity of *Fpn1^{Cdh5}-cKO* and APP/PS mice. The distribution and expression of FtH and FtL were detected by immunohistochemistry (IHC); the representative IHC results of FtH and FtL staining in the SCN and cortex regions are shown in (A). Scale bar = 50 μ m. (B, C) Quantitative analysis of the protein intensities of FtH and FtL in the SCN and cortex regions from two separate fields for each mouse. The data are presented as the mean \pm SEM, $n=3$. (D) Hippocampal FtH and FtL proteins, as evaluated by western blot analysis. (E) Quantitative analysis of FtH and FtL protein levels from the western blot data, compared to the *Fpn1^{flox/flox}* group, after normalizing to the respective β -actin expression. The data are presented as the mean \pm SEM, $n=3$. The locomotor activities of the mice were measured using a Mouse Wheel Running Activity Monitoring System. The monitoring data represent the distance traveled for each animal per second (cm/s). (F, I) Representative double-plotted actograms of spontaneous locomotor activity of *Fpn1^{flox/flox}* and *Fpn1^{Cdh5}-cKO* mice (F) or WT (control) and APP/PS1 mice (I) that were kept in a standard photoperiod of 12 h light (L) and 12 h dark (D) for 6 days, followed by 48 h of constant darkness. In these plots, black bars indicate activity and gray boxes indicate periods of darkness. (G) Average autonomous activities of the *Fpn1^{flox/flox}* and *Fpn1^{Cdh5}-cKO* mice from 12:00 a.m. to 12:00 p.m. (H) Total activity of the *Fpn1^{flox/flox}* and *Fpn1^{Cdh5}-cKO* mice per day during the experimental period. (J, K) Daily (J) and total (K) activities for the WT and APP/PS1 mice. (L, M) Serum melatonin levels in the indicated groups. All the data are presented as the mean \pm SEM. The numbers of mice (n) for each group are indicated in (G, H), (J, K), and (L, M). Statistical analysis was performed using a two-tailed Student's t -test; * $p < 0.05$, ** $p < 0.01$, *** $p < 0.001$, compared with the *Fpn1^{flox/flox}* group or the WT group.

To examine whether iron supplementation can shift clock gene expression in the opposite direction of that observed upon chelation, we treated the U251 cells with FAC. As expected, the protein level of PER1 was increased, while CLOCK protein was diminished compared to the control cells. We did not see significant changes in the expression of BMAL1 and phosphorylated GSK3 β (Figure 3G–J).

In order to validate the results obtained from U251 cells, we utilized the MA-c cell line and performed a qRT-PCR assay to examine the mRNA expression pattern of clock genes, including *Bmal1*, *Clock*, *Per1*, and *Cry1*. The mRNA results demonstrate that the expression of clock genes in mouse MA-c cells maintained circadian rhythmicity, which is in contrast to the mRNA results obtained from human U251 cells (Figure S4). Additionally, we investigated the impact of altered cellular iron levels on the protein expression of *Per1*, at 8:00 a.m. and 10:00 p.m., in MA-c cells (Figures S5 and S6). The findings in MA-c cells reveal that the addition of FAC enhanced *PER1* expression, while DFO inhibited it. Collectively, these results in MA-c cells further support a potential molecular connection between cellular iron and *PER1* expression. Taken together, our results show that altered iron levels influence the expression of the core clock genes, including *PER1*, *CLOCK*, and *BMAL1*, in vitro.

3.4 | Endogenous overexpression of FPN1 and TfR1 induces changes in cellular iron levels in U251 cells

To support our hypothesis that altered cellular iron levels influence the expression of clock genes, we constructed two cell models that endogenously overexpress FPN1 (U251-FPN1) or TfR1 (U251-TfR1). In the process of cellular iron transport, TfR1 is the gateway for import of iron into cells. As expected, overexpression of TfR1 induced enhanced iron import and subsequent iron accumulation in U251 cells, while the U251-FPN1 cells exhibited lower cellular iron content, as evidenced by increased FtH and FtL expression in the U251-TfR1 cells and decreased protein levels of FtH and FtL in the U251-FPN1 cells (Figure 4).

3.5 | The levels of PER1, CLOCK, and BMAL1 proteins are altered in U251-FPN1 and U251-TfR1 cells

Next, we assessed the levels of *PER1*, *PER2*, *BMAL1*, and *CLOCK* in the U251-FPN1 and U251-TfR1 cells. In the U251-FPN1 cells, we observed considerably reduced expression of *PER1* and *PER2*, while, accordingly, the levels of *CLOCK* and *BMAL1* were increased (Figure 5A–D). This effect is likely to have occurred via elevated levels of p-GSK3 β in the cells (Figure 5E,F). These results align with those we observed following iron chelation. In the U251-TfR1 cells, with their elevated cellular iron status, the levels of *PER1* and *PER2* were increased, while the *CLOCK* and *BMAL1* proteins were decreased. However, we did not observe measurable alterations in p-GSK3 β levels (Figure 5G–L). These results from U251-TfR1 cells are consistent with the results in U251 cells treated with FAC. Our results further strengthen the hypothesis that the expression of core clock genes can be regulated by altered cellular iron levels.

3.6 | The mechanism of iron regulation of circadian rhythms may be via changes in PER1

The above results indicate that decreased cellular iron can cause a decline in the levels of *PER1*, which in turn leads to elevated expression of *CLOCK*, which is down-regulated by *PER1*. Therefore, we conjectured that *PER1* is directly influenced by cellular iron levels. To test this, we increased *PER1* levels in U251-FPN1 cells through transfection with a plasmid-overexpressing *PER1* (*Per1*-OE). In U251-FPN1 cells with *PER1* overexpression, we detected a decreased trend in *CLOCK* protein levels, although the difference was not statistically significant (Figure 6A,B). On the other hand, we also decreased *PER1* levels in U251-TfR1 cells via *Per1*-shRNAs. After shRNA knockdown of *Per1*, *CLOCK* protein levels were significantly increased compared to the controls (Figure 6C–E), suggesting that the mechanism of iron's effect on the TTFL may be through changes in *PER1* protein levels.

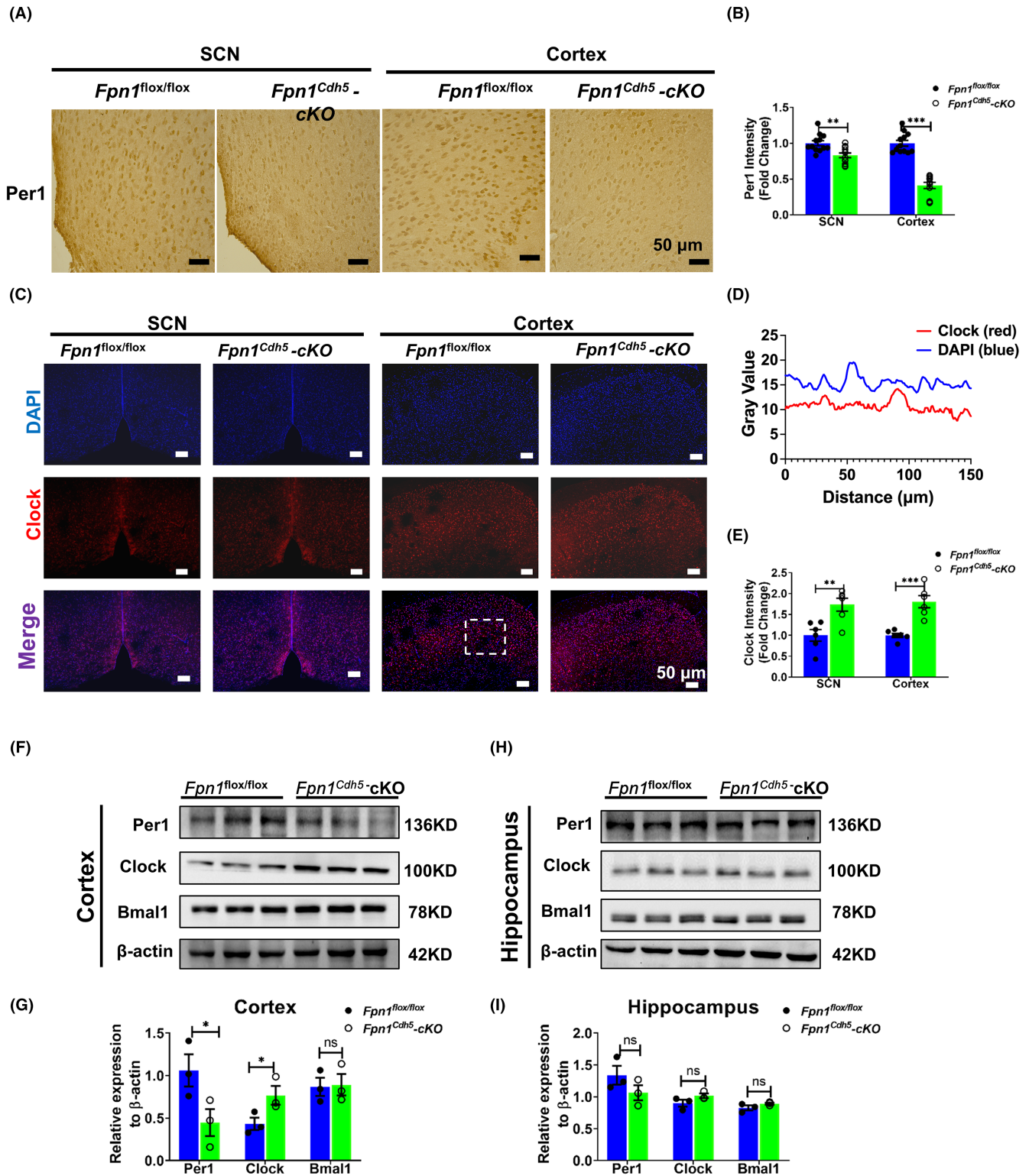


FIGURE 2 Distribution and expression of Per1 and Clock in the SCN, cortex, and hippocampus regions of *Fpn1*^{flox/flox} and *Fpn1*^{Cdh5-cKO} mice. (A) Per1 distribution in the SCN and cortex, as detected by IHC. (B) Average intensity of Per1 in these regions, for each mouse. The data were calculated from four separate fields. The data are presented as the mean \pm SEM, $n=3$. Scale bar = 50 μ m. (C) Double-immunofluorescence assays were performed to detect the distribution and expression of Clock in the SCN and cortex. Scale bar = 50 μ m. (D) The intensity profile (dashed box in panel C) of the signals from both fluorescent channels indicates the colocalization of Clock and DAPI. (E) Quantified average intensity of Clock in the SCN and Cortex regions from two separate fields for each mouse. The data are presented as the mean \pm SEM, $n=3$. (F–I) Representative western blots for the expression levels of Per1, Clock, and Bmal1 in the cortex (F) and hippocampus (H) and quantification of the western blot analysis results in the cortex (G) and hippocampus (I). The data are presented as the mean \pm SEM, $n=3$. Statistical analysis was performed using a two-tailed Student's *t*-test; * $p < 0.05$, ** $p < 0.01$, *** $p < 0.001$, compared with the *Fpn1*^{flox/flox} group, "ns" refers to no significance.

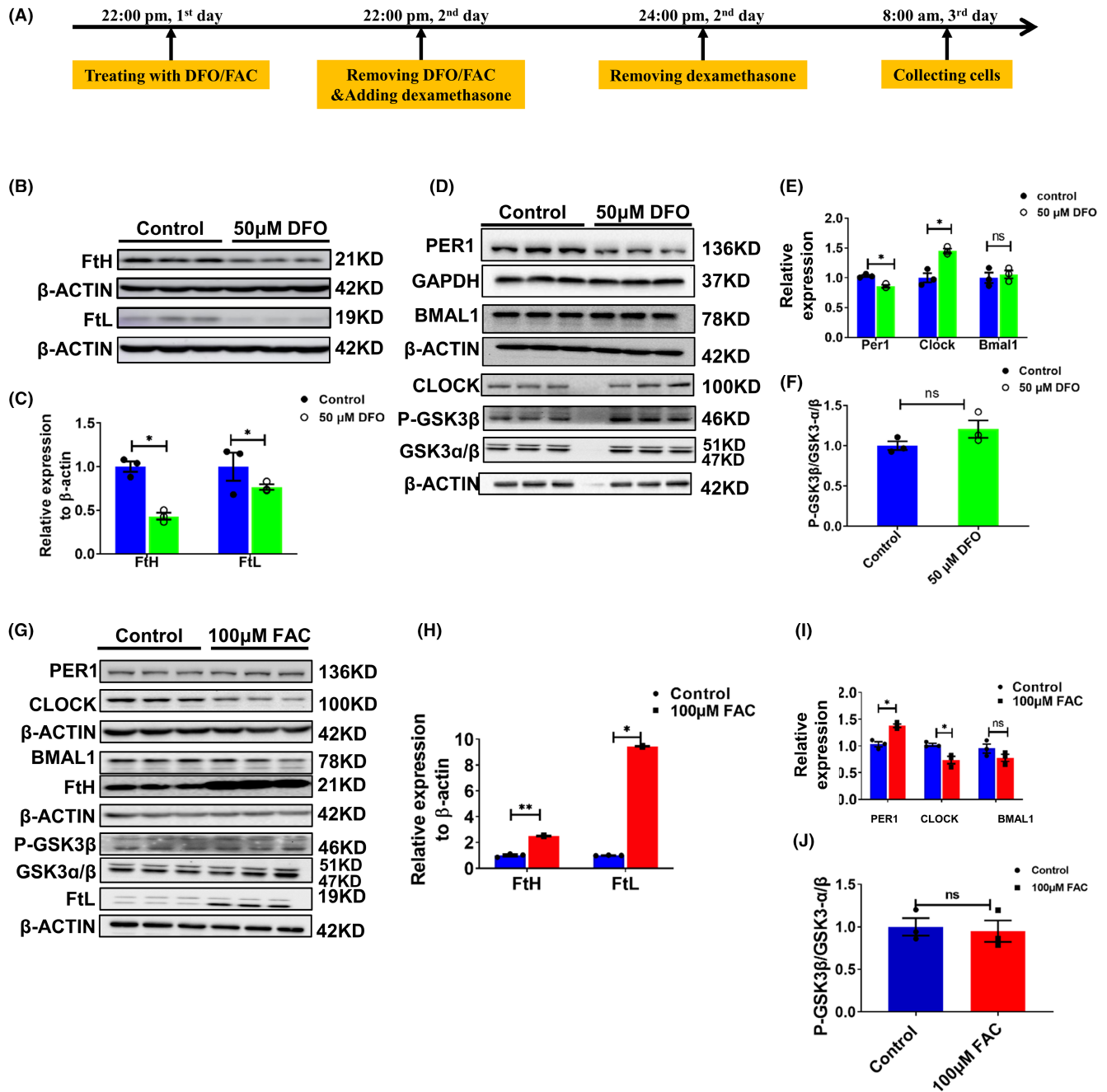


FIGURE 3 Altered expression of PER1, CLOCK, BMAL1 and P-GSK3 β in U251 cells treated with 50 μ M DFO or 100 μ M FAC at 8 am. (A) Schematic illustration of the treatment of cells with DFO or FAC; the cells were collected and detected at 8 a.m. (B) Representative western blot analysis results for FtH and FtL in U251 cells treated with 50 μ M DFO. (C) Statistical analysis of the results from the experiment presented in panel B. FtH and FtL were compared to the control group after normalizing to the respective β -ACTIN expression. (D) Protein levels of PER1, CLOCK, BMAL1 and p-GSK3 β , as detected by western blot analysis. (E) Statistical analysis of the results of the experiment shown in panel D. (F) Statistical analysis of phosphorylated GSK3 β levels. The data represented in panels E and F were quantified after normalizing to the respective GAPDH or β -ACTIN expression. (G) Representative western blot analysis results for PER1, CLOCK, BMAL1, FtH, p-GSK3 β , GSK3 α/β and FtL, as detected by western blot analysis, in U251 cells treated with 100 μ M FAC for 24 h. (H) Statistical analysis of FtH and FtL compared to the control group after normalizing to the respective β -ACTIN expression. (I) Quantification of the results of PER1, CLOCK, and BMAL1 protein expression. (J) Statistical analysis of P-GSK3 β levels. The data represented in panels I and J were quantified after normalizing to β -ACTIN expression. The data are presented as the mean \pm SEM, $n=3$. Statistical analysis was performed using a two-tailed Student's *t*-test; * $p < 0.05$, ** $p < 0.01$ compared to the Control group. "ns" refers to no significance.

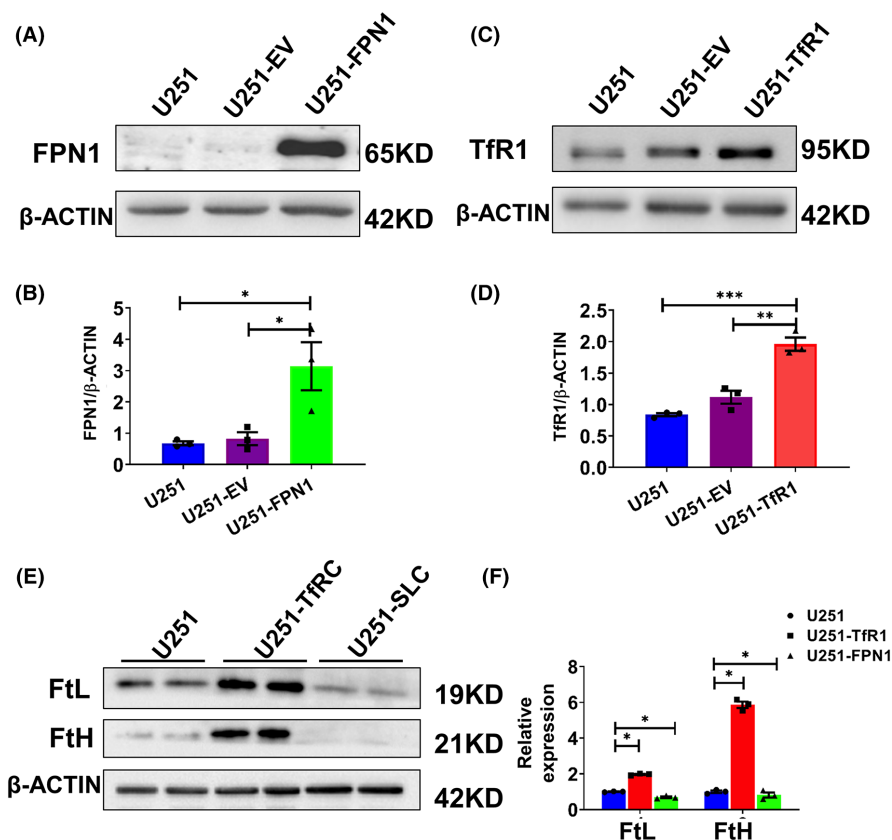


FIGURE 4 Construction and verification of U251 cells endogenously overexpressing FPN1 and TfR1. After generating U251 cells stably overexpressing FPN1 or TfR1, we evaluated the protein levels of FPN1 and TfR1 by western blot analysis. (A, C) Western blot analysis results for FPN1 and TfR1 in U251, U251 cells transfected with empty vector (U251-EV), and U251 cells overexpressing FPN1 (U251-FPN1) or TfR1 (U251-TfR1). (B, D) Quantification of the results of the experiments presented in panels A and C. The protein levels were normalized to β -ACTIN expression. The data are presented as the mean \pm SEM, $n=3$. Statistical analysis was performed using a two-tailed Student's *t*-test; * $p < 0.05$, ** $p < 0.01$, *** $p < 0.001$. (E) Western blot analysis results for FtL and FtH expression in U251-TfR1 and U251-FPN1 cells. (F) Statistical analysis for FtH and FtL compared to the U251 group after normalizing to the respective β -ACTIN expression. The data are presented as the mean \pm SEM, $n=3$. Statistical analysis was performed using a two-tailed Student's *t*-test; * $p < 0.05$.

4 | CONCLUSION

Aging is characterized by progressive impairments in physiological functions in the body, including the robustness of the circadian clock, that can lead to disturbed sleep-wake cycles and lowered synchronization of circadian rhythms, which in turn accelerates the process of aging.^{33,36} Numerous studies have examined the pathogenesis of aging-related circadian rhythm disruption, including disturbances in the autonomic nervous system, hormone levels, or immune system.³⁷⁻³⁹ However, the underlying cause(s) of the changes to the circadian rhythm with age largely remain enigmatic. As one of the most abundant trace elements in the brain, iron contributes to various essential physiological processes, including oxygen transport, DNA synthesis, and oxidative phosphorylation.¹⁰ Numerous studies have shown that progressive iron accumulation is a major risk factor in aging and is connected to neurodegenerative diseases, such as AD and PD.^{29,40,41} Aberrant brain iron increases with age, resulting in dysfunction of the central nervous system, since iron-induced redox stress can accelerate cellular senescence and neurodegeneration. It has also been found that excessive iron accumulation is usually

accompanied by sleep-wake phase disorders, which are closely related to the circadian rhythm.^{42,43} Yet, the apparent relationship between elevated brain iron levels and circadian clock desynchrony in the elderly, and the mechanisms underlying these effects, represent a gap in our knowledge.

In the present study, we explored whether altered brain iron levels can lead to changes in behavioral rhythm, and the mechanisms involved. In our study, we used *Fpn1*^{Cdh5}-cKO mice as a model of brain iron deficiency since conditional knock of *Fpn1* in microvascular endothelial cells blocks iron import into the brain through the BBB.²⁰ In addition, previous studies have reported elevated iron levels in the cortex and hippocampus of APP/PS1 mice.^{21,29} In our present study, *Fpn1*^{Cdh5}-cKO mice exhibited enhanced activity rhythms, while APP/PS1 inhibited activities. It is worth noting that the observed changes in locomotor activity rhythms in the APP/PS1 mice with brain iron overload are consistent with a previous study.⁴⁴ In this study, we assessed the levels of the cellular iron storage proteins, namely FtH and FtL, in various brain regions, including the SCN, cortex, and hippocampus, of the *Fpn1*^{Cdh5}-cKO mice. We found that these proteins were decreased compared to age-matched controls, which is consistent with lower

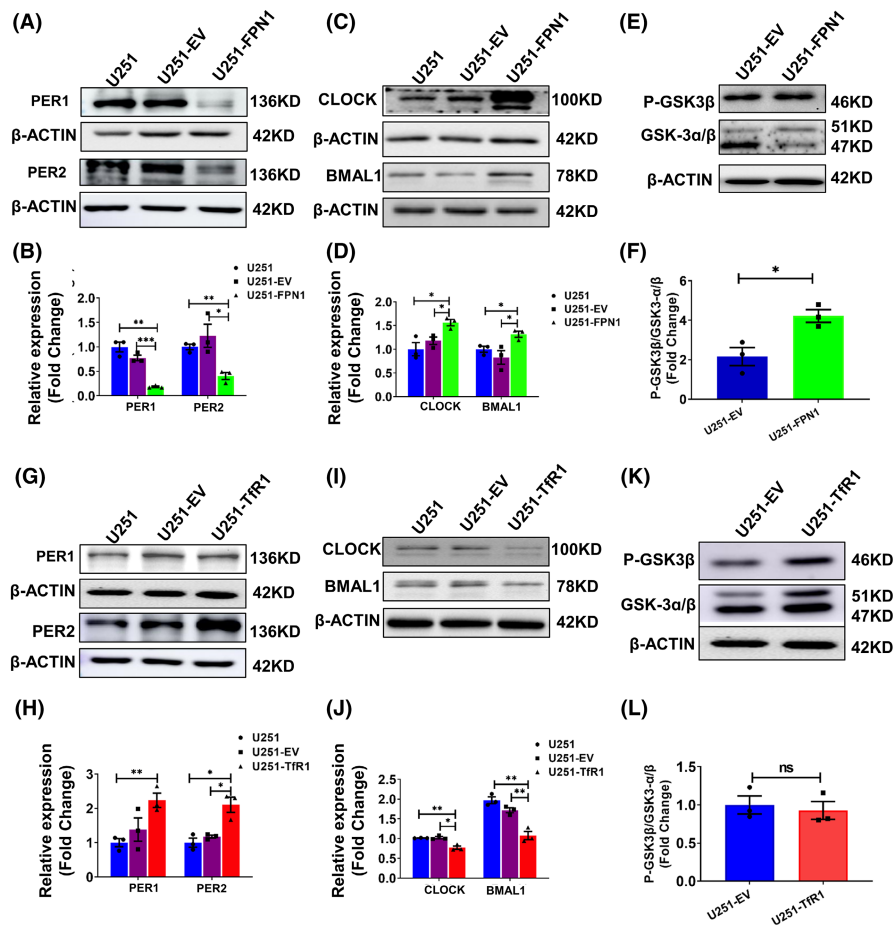


FIGURE 5 Protein levels of PER1, PER2, CLOCK, BMAL1, and p-GSK3 β in U251-FPN1 and U251-TfR1 cells. (A) Western blot analysis results for PER1, PER2 in U251 cells, U251 cells with empty vector (U251-EV), and U251 cells overexpressing FPN1 (U251-FPN1). (C) Representative western blot analysis of CLOCK and BMAL1 in these three groups. (E) Levels of phosphorylated GSK3 β and GSK-3 α/β in the U251-EV and U251-FPN1 groups. (B, D, F) Statistical analysis of the expression of the indicated proteins compared to the U251 or U251-EV group after normalizing to the respective β -ACTIN expression. The data are presented as the mean \pm SEM, $n = 3$. (G, I) Representative western blot analysis results for PER1, PER2, BMAL1, and CLOCK in U251, U251-EV, and U251 cells overexpressing TfR1 (U251-TfR1). (K) Levels of phosphorylated GSK3 β in the indicated groups. (H, J, L) Statistical analysis for the indicated proteins compared to the U251 or U251-EV group after normalizing to the respective β -ACTIN expression. The data are presented as the mean \pm SEM, $n = 3$. Statistical analysis was performed using a two-tailed Student's t -test; $*p < 0.05$, $**p < 0.01$, "ns" refers to no significance.

uncommitted iron levels in these brain regions. The increased FtH and FtL levels have already been reported in our previous study. Since both of these mouse models exhibited disturbances in locomotor rhythm (Figure 1), we conclude that there is a connection between iron levels and the regulation of circadian rhythms.

There has been robust study on melatonin and circadian rhythms. Melatonin is not only examined with respect to its effects on circadian rhythms but also various other functions, such as antioxidant effects.^{30,31} A series of studies have demonstrated that melatonin can alleviate neural damage and cell death caused by excessive iron.^{45,46} In the present study, we observed a significant increase in serum melatonin levels in APP/PS1 mice, while *Fpn1*^{cdh5-cKO} mice with brain iron deficiency showed the opposite trend. This result suggests a potential correlation between brain iron levels and melatonin levels. More importantly, it implies that elevated brain iron in APP/PS1 mice may lead to increased oxidative stress levels,

triggering a negative feedback mechanism to release melatonin. This hypothesis still requires further experimental validation, but it is consistent with our findings that brain iron has a significant role in regulating circadian rhythms.

In order to further understand the effects of brain iron on the shifts in the circadian rhythm, we evaluated the expression of core clock genes, including PER1, CLOCK, and BMAL1 in the SCN, cortex, and hippocampus in 10-month-old *Fpn1*^{cdh5-cKO} mice. We observed a diminished expression of PER1 and increased CLOCK expression in the SCN and cortex regions compared to controls, suggesting that brain iron status can have an influence on the expression of clock genes. Several previous studies revealed that peripheral iron accumulation plays a key role in aging-related shifts of circadian function; sleep disturbances have been frequently seen in iron overload-related diseases.^{47,48} On the other hand, iron supplementation in young mice (4-week-old) yields indistinguishable or altered

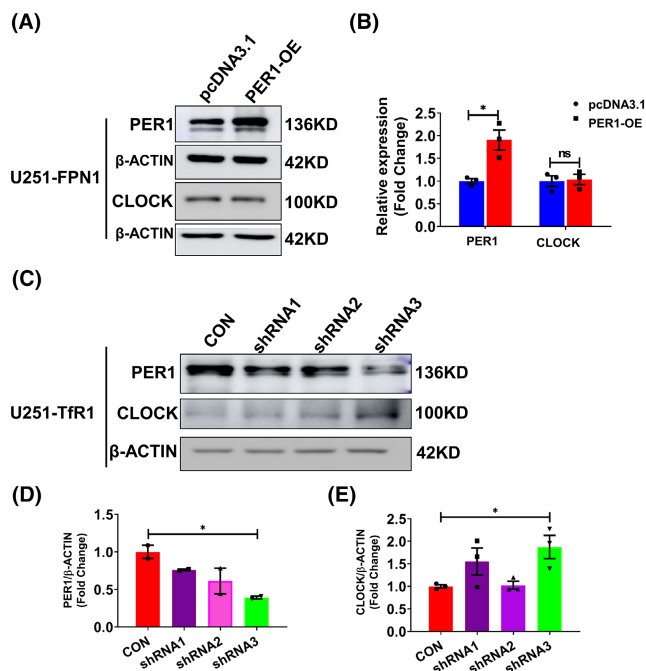


FIGURE 6 Expression levels of CLOCK protein in U251-FPN1 and U251-TfR1 cells with modified Per1 expression. (A) Representative western blot analysis results of PER1 and CLOCK in U251-FPN1 cells overexpressing PER1. (B) Quantification of the experiment presented in panel A. The data are presented as the mean \pm SEM after normalizing to the respective β -ACTIN expression, $n=3$. (C) Western blot analysis results of PER1 and CLOCK proteins in U251-TfR1 cells with inhibited expression of PER1 using *Per1*-shRNAs. (D, E) Quantified results of PER1 and CLOCK expression from the experiment shown in panel C. The data are presented as the mean \pm SEM after normalizing to the respective β -ACTIN expression. $n=3$, $*p < 0.05$, "ns" refers to no significance.

expression of *Per1* and *Per2* in the liver.¹⁸ Some additional studies have aimed to connect iron metabolism and circadian rhythms. The autophagy-mediated degradation of BMAL1 favors lipid peroxidation and cell death in human tumor cell lines.⁴⁹ Dietary iron may affect circadian glucose production through heme synthesis, which has also been demonstrated to modulate liver PER1 and PER2 expression in mice.^{50,51} Heme can also function as a cofactor of clock genes and thus regulate biological cycles.^{52,53} In addition, iron accumulation can also affect the expression of core clock genes, including PER1 and PER2, through histone methylation.¹⁸ In the present study, we found that changes in brain iron status can influence the expression of PER1, CLOCK, and BMAL1 in various brain regions of 10-month-old mice. Together, our results suggest that iron accumulation may drive disturbances in circadian and locomotor activity rhythms.

Astrocytes can act as active participants in the SCN network and display robust rhythms and TTFL function. Moreover, the astrocytic TTFL clock in the SCN is sufficient to determine behavioral rhythms.⁵⁷ In contrast, disruption of the astrocytic TTFL lengthens behavioral and ex vivo SCN periods.^{55,56} Using the U251 glioma cell model, we also observed rhythmic transcriptions of the clock genes,

including *BMAL1*, *CLOCK*, *CRY1*, and *PER1*, which adds novel evidence that the biological clock also functions in vitro,⁵⁴ suggesting that this cell line is suitable for biological rhythm research.

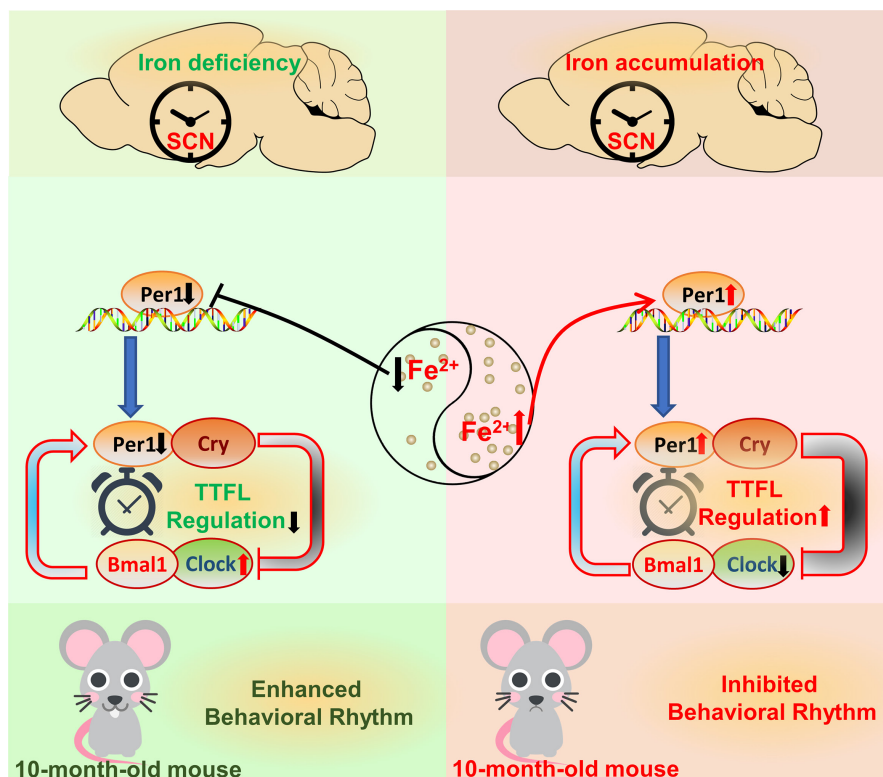
In the present study, we treated U251 cells with the iron chelator DFO to deplete the cells of iron and mimic the in vivo iron-starvation state. Furthermore, we constructed FPN1-overexpressing U251 cells (U251-FPN1) to generate an iron-depleted phenotype. We then assessed the protein levels of PER1, CLOCK, and BMAL1, since in mammalian cells, the BMAL1-CLOCK heterodimer can drive the transcription of *Per* and *Cry1*. The PER-CRY1 protein complexes then translocate into the nucleus and suppress CLOCK-BMAL1 activity. Additionally, we also investigated the phosphorylation of GSK3 β , as p-GSK3 β pathway has been reported to down-regulate Bmal1 expression.^{5,34,35} We found up-regulated protein levels of p-GSK3 β and decreased PER1 levels in the two iron-deficient cell models. In contrast, p-GSK3 β and *Per1* showed an opposite expression pattern in both FAC-treated U251 cells and U251-TfR1 cells that overexpress TfR1 and take up erroneously elevated amounts of iron.

The mRNA expression of the core clock genes, including PER1, CLOCK, BMAL1, and CRY1, in U251 cells exhibited rhythmicity, as indicated in Figure S1. Therefore, it is reasonable to suspect that the influence of altered cellular iron on the expression of these genes will be affected by the time point of cell collection. However, our findings demonstrate that the protein expression of PER1, CLOCK, and BMAL1 detected at 8:00 p.m. (Figure S3) is similar to that observed at 8:00 a.m. The data presented in Figure 3 from U251 cells suggest that cellular iron accumulation induced by FAC promotes the expression of PER1, while iron starvation caused by DFO chelation inhibits PER1 expression. It is noteworthy that the impact of iron on the expression of clock genes remains consistent, regardless of the time at which the cells are collected and subsequently measured. In our study, we also observed rhythmic mRNA expression of *Per1*, *Clock*, *Bmal1*, and *Cry1* in a mouse cell line, MA-c. Moreover, the effects of cellular iron levels on the expression of *Per1* are consistent across different time points of cell collection and subsequent measurement in MA-c cells.

Considering all of these above results, we conjecture that PER1 plays a vital role as a key clock gene in the process of iron regulation of the biological rhythm. To further investigate this hypothesis, we examined the expression of CLOCK protein levels in U251-FPN1 cells overexpressing PER1. Under these conditions, CLOCK protein levels were decreased. In contrast, knockdown of *Per1* using shRNA in U251-TfR1 cells significantly increased the levels of CLOCK protein. These findings suggest that PER potentially acts as a molecular mediator of the shifted circadian rhythm induced by altered iron levels. Taken together, our in vitro data from human and mouse cell lines indicate that elevated cellular iron levels may disrupt the cellular circadian rhythm by positively regulating PER1 expression. These in vitro findings further reinforce and validate the conclusions drawn from the mouse brain experiments with altered brain iron status, as presented in Figures 1 and 2.

In summary, our study demonstrates that altered brain iron levels can affect the expression of clock genes in the brain, ultimately

FIGURE 7 Schematic representation of the proposed molecular mechanism of diverse brain iron levels in circadian clock regulation. Decreased brain iron levels can inhibit the expression of Per1, which further inhibits TTFL regulation, resulting in elevated Clock protein and an enhancement of the behavioral rhythm. On the contrary, accumulated iron can induce increased Per1 level, therefore strengthening TTFL regulation, finally inhibiting rhythmic activity.



resulting in abnormal biological rhythm. Decreased cellular iron levels can inhibit the expression of PER1, which further inhibits TTFL regulation, resulting in elevated CLOCK protein and an enhancement of the behavioral rhythm. In contrast, iron accumulation induced increased PER1, strengthening TTFL regulation and therefore inhibiting rhythmic activity (Figure 7). PER1 may be a crucial clock gene mediating the shifted circadian rhythm during this process, however, mechanistic details require further investigation. Our study helps to close the gap in our understanding of age-related dysregulation of the circadian rhythm and identifies brain iron regulation as a novel target for combating age-associated disturbances of circadian rhythm.

ACKNOWLEDGMENTS

This research was funded by the project of Hebei Research Center of the Basic Discipline of Cell Biology (C2023205049), the Natural Science Foundation of Hebei Province (C2023423008 and H2019423032), the Science Research Project of Hebei Education Department (BJK2023095), the National Natural Science Foundation of China (32070962), and the Basic research program for young teachers of Hebei University of Chinese Medicine (grant number: YQ2018007).

CONFLICT OF INTEREST STATEMENT

The authors declare that they have no conflicts of interest.

DATA AVAILABILITY STATEMENT

Data from this study are available from the corresponding author, Yan-Zhong Chang and Peng Yu, upon reasonable request.

ORCID

Yan-Zhong Chang  <https://orcid.org/0000-0002-6386-9649>

REFERENCES

- Hoyt KR, Obrietan K. Circadian clocks, cognition, and Alzheimer's disease: synaptic mechanisms, signaling effectors, and chronotherapeutics. *Mol Neurodegener.* 2022;17:35.
- Liu PY, Reddy RT. Sleep, testosterone and cortisol balance, and ageing men. *Rev Endocr Metab Disord.* 2022;23:1323-1339.
- Mehra R, Chung MK, Olshansky B, et al. Sleep-disordered breathing and cardiac arrhythmias in adults: mechanistic insights and clinical implications: a scientific Statement from the American Heart Association. *Circulation.* 2022;146:e119-e136.
- Nassan M, Videnovic A. Circadian rhythms in neurodegenerative disorders. *Nat Rev Neurol.* 2022;18:7-24.
- Castro-Zavala A, Alegre-Zurano L, Cantacorps L, et al. Bmal1-knockout mice exhibit reduced cocaine-seeking behaviour and cognitive impairments. *Biomed Pharmacother.* 2022;153:113333.
- Logan RW, McClung CA. Rhythms of life: circadian disruption and brain disorders across the lifespan. *Nat Rev Neurosci.* 2019;20:49-65.
- Meng D, Yang M, Hu L, et al. Rifaximin protects against circadian rhythm disruption-induced cognitive impairment through preventing gut barrier damage and neuroinflammation. *J Neurochem.* 2022;163:406-418.
- Zhang Y, Liu L, Zhao X, Yan S, Zeng F, Zhou D. New insight into ischemic stroke: circadian rhythm in post-stroke angiogenesis. *Front Pharmacol.* 2022a;13:927506.
- Neves AR, Albuquerque T, Quintela T, Costa D. Circadian rhythm and disease: relationship, new insights, and future perspectives. *J Cell Physiol.* 2022;237:3239-3256.
- Ward RJ, Dexter DT, Crichton RR. Iron, Neuroinflammation and neurodegeneration. *Int J Mol Sci.* 2022;23:7267.
- Qian ZM, Ke Y. Brain iron transport. *Biol Rev Camb Philos Soc.* 2019;94:1672-1684.

12. Sun Y, Xia X, Basnet D, Zheng JC, Huang J, Liu J. Mechanisms of Ferroptosis and emerging links to the pathology of neurodegenerative diseases. *Front Aging Neurosci.* 2022;14:904152.
13. Ward RJ, Zucca FA, Duyn JH, Crichton RR, Zecca L. The role of iron in brain ageing and neurodegenerative disorders. *Lancet Neurol.* 2014;13:1045-1060.
14. Blacher E, Tsai C, Litichevskiy L, et al. Aging disrupts circadian gene regulation and function in macrophages. *Nat Immunol.* 2022;23:229-236.
15. Musiek ES, Holtzman DM. Mechanisms linking circadian clocks, sleep, and neurodegeneration. *Science.* 2016;354:1004-1008.
16. Holth JK, Fritschi SK, Wang C, et al. The sleep-wake cycle regulates brain interstitial fluid tau in mice and CSF tau in humans. *Science.* 2019;363:880-884.
17. Lauretti E, Di Meco A, Merali S, Pratico D. Circadian rhythm dysfunction: a novel environmental risk factor for Parkinson's disease. *Mol Psychiatry.* 2017;22:280-286.
18. Liu J, Zhao Y, Ding Z, et al. Iron accumulation with age alters metabolic pattern and circadian clock gene expression through the reduction of AMP-modulated histone methylation. *J Biol Chem.* 2022;298:101968.
19. Ishii T, Warabi E, Mann GE. Circadian control of BDNF-mediated Nrf2 activation in astrocytes protects dopaminergic neurons from ferroptosis. *Free Radic Biol Med.* 2019;133:169-178.
20. You L, Yu PP, Dong T, et al. Astrocyte-derived hepcidin controls iron traffic at the blood-brain-barrier via regulating ferroportin 1 of microvascular endothelial cells. *Cell Death Dis.* 2022;13:667.
21. Xu Y, Zhang Y, Zhang JH, et al. Astrocyte hepcidin ameliorates neuronal loss through attenuating brain iron deposition and oxidative stress in APP/PS1 mice. *Free Radic Biol Med.* 2020;158:84-95.
22. Marzoll D, Serrano FE, Shostak A, Schunke C, Diernfellner ACR, Brunner M. Casein kinase 1 and disordered clock proteins form functionally equivalent, phospho-based circadian modules in fungi and mammals. *Proc Natl Acad Sci U S A.* 2022;119:e2118286119.
23. Smyllie NJ, Bagnall J, Koch AA, et al. Cryptochrome proteins regulate the circadian intracellular behavior and localization of PER2 in mouse suprachiasmatic nucleus neurons. *Proc Natl Acad Sci U S A.* 2022;119:e2116845119.
24. Sullivan KA, Grant CV, Jordan KR, Obrietan K, Pyter LM. Paclitaxel chemotherapy disrupts behavioral and molecular circadian clocks in mice. *Brain Behav Immun.* 2022;99:106-118.
25. Zhen Y, Xi Z, Hu L, et al. Impacts of circadian gene Period2 knockout on intestinal metabolism and hepatic antioxidant and inflammation state in mice. *Oxid Med Cell Longev.* 2022;2022:7896371.
26. Li Z, Lan Y, He W, et al. Mouse embryonic head as a site for hematopoietic stem cell development. *Cell Stem Cell.* 2012;11:663-675.
27. You LH, Li Z, Duan XL, Zhao BL, Chang YZ, Shi ZH. Mitochondrial ferritin suppresses MPTP-induced cell damage by regulating iron metabolism and attenuating oxidative stress. *Brain Res.* 2016;1642:33-42.
28. Wu Q, Hao Q, Li H, et al. Brain iron deficiency and affected contextual fear memory in mice with conditional Ferroportin1 ablation in the brain. *FASEB J.* 2021;35:e21174.
29. Zhang Y, Bai X, Zhang Y, et al. Hippocampal iron accumulation impairs synapses and memory via suppressing Furin expression and down-regulating BDNF maturation. *Mol Neurobiol.* 2022b;59:5574-5590.
30. Cajochen C, Kräuchi K, Wirz-Justice A. Role of melatonin in the regulation of human circadian rhythms and sleep. *J Neuroendocrinol.* 2003;15:432-437.
31. Reiter RJ, Mayo JC, Tan DX, Sainz RM, Alatorre-Jimenez M, Qin L. Melatonin as an antioxidant: under promises but over delivers. *J Pineal Res.* 2016;61:253-278.
32. Lee J, Sul HJ, Choi H, Oh DH, Shong M. Loss of thyroid gland circadian PER2 rhythmicity in aged mice and its potential association with thyroid cancer development. *Cell Death Dis.* 2022;13:898.
33. Zhu Y, Liu Y, Escames G, et al. Deciphering clock genes as emerging targets against aging. *Ageing Res rev.* 2022;81:101725.
34. Guo R, Zhao B, Wang Y, et al. Cichoric acid prevents free-fatty-acid-induced lipid metabolism disorders via regulating Bmal1 in hepG2 cells. *J Agric Food Chem.* 2018;66:9667-9678.
35. Lee SB, Park J, Kwak Y, et al. Disrupted-in-schizophrenia 1 enhances the quality of circadian rhythm by stabilizing BMAL1. *Transl Psychiatry.* 2021;11:110.
36. Welz PS, Benitah SA. Molecular connections between circadian clocks and aging. *J Mol Biol.* 2020;432:3661-3679.
37. Buijs RM, Escobar C, Swaab DF. The circadian system and the balance of the autonomic nervous system. *Handb Clin Neurol.* 2013;117:173-191.
38. He R, Zhang S, Yu J, et al. Per1/Per2 knockout affects spleen immune function in elderly mice via inducing spleen lymphocyte Ferroptosis. *Int J Mol Sci.* 2022;23:12962.
39. Musiek ES, Xiong DD, Holtzman DM. Sleep, circadian rhythms, and the pathogenesis of Alzheimer disease. *Exp Mol Med.* 2015;47:e148.
40. Gao X, Wang Z, Xiong L, et al. The bs-YHEDA peptide protects the brains of senile mice and thus recovers intelligence by reducing iron and free radicals. *Free Radic Biol Med.* 2022;190:216-225.
41. Kwon K, Cho H, Lee S, et al. Adaptive cellular response of the substantia nigra dopaminergic neurons upon age-dependent iron accumulation. *Ageing Cell.* 2022;21:e13694.
42. Lancione M, Donatelli G, Del Prete E, et al. Evaluation of iron overload in nigrosome 1 via quantitative susceptibility mapping as a progression biomarker in prodromal stages of synucleinopathies. *Neuroimage.* 2022;260:119454.
43. Sahu M, Tripathi R, Jha NK, Jha SK, Ambasta RK, Kumar P. Cross talk mechanism of disturbed sleep patterns in neurological and psychological disorders. *Neurosci Biobehav Rev.* 2022;140:104767.
44. Castro-Caraballo F, Suarez-Roca H, Estevez J, Bonilla E. Spontaneous motor activity in mice overloaded with iron-dextran. *Invest Clin.* 1992;33:121-134.
45. Gao Y, Wang T, Cheng Y, et al. Melatonin ameliorates neurological deficits through MT2/IL-33/ferritin H signaling-mediated inhibition of neuroinflammation and ferroptosis after traumatic brain injury. *Free Radic Biol Med.* 2023;199:97-112.
46. Zhang D, Jia X, Lin D, Ma J. Melatonin and ferroptosis: mechanisms and therapeutic implications. *Biochemical Pharmacology.* 2023;218:115909.
47. Tarasiuk A, Abdul-Hai A, Moser A, Freidman B, Tal A, Kapelushnik J. Sleep disruption and objective sleepiness in children with beta-thalassemia and congenital dyserythropoietic anemia. *Arch Pediatr Adolesc Med.* 2003;157:463-468.
48. Wallen GR, Minniti CP, Krumlauf M, et al. Sleep disturbance, depression and pain in adults with sickle cell disease. *BMC Psychiatry.* 2014;14:207.
49. Yang M, Chen P, Liu J, et al. Clockophagy is a novel selective autophagy process favoring ferroptosis. *Sci Adv.* 2019;5:eaaw2238.
50. Kaasik K, Lee CC. Reciprocal regulation of haem biosynthesis and the circadian clock in mammals. *Nature.* 2004;430:467-471.
51. Simcox JA, Mitchell TC, Gao Y, et al. Dietary iron controls circadian hepatic glucose metabolism through heme synthesis. *Diabetes.* 2015;64:1108-1119.
52. Kitanishi K, Igarashi J, Hayasaka K, et al. Heme-binding characteristics of the isolated PAS-A domain of mouse Per2, a transcriptional regulatory factor associated with circadian rhythms. *Biochemistry.* 2008;47:6157-6168.
53. Raghuram S, Stayrook KR, Huang P, et al. Identification of heme as the ligand for the orphan nuclear receptors REV-ERBalpha and REV-ERBbeta. *Nat Struct Mol Biol.* 2007;14:1207-1213.
54. Abe YO, Yoshitane H, Kim DW, et al. Rhythmic transcription of Bmal1 stabilizes the circadian timekeeping system in mammals. *Nat Commun.* 2022;13:4652.
55. Brancaccio M, Patton AP, Chesham JE, Maywood ES, Hastings MH. Astrocytes control circadian timekeeping in the Suprachiasmatic nucleus via glutamatergic signaling. *Neuron.* 2017;93:1420-1435.e5.

56. Brancaccio M, Edwards MD, Patton AP, et al. Cell-autonomous clock of astrocytes drives circadian behavior in mammals. *Science*. 2019;363:187-192.
57. Patton AP, Smyllie NJ, Chesham JE, Hastings MH. Astrocytes sustain circadian oscillation and bidirectionally determine circadian period, but do not regulate circadian phase in the suprachiasmatic nucleus. *J Neurosci*. 2022;42:5522-5537.

How to cite this article: Wu Q, Ren Q, Wang X, et al. Cellular iron depletion enhances behavioral rhythm by limiting brain Per1 expression in mice. *CNS Neurosci Ther*. 2024;30:e14592. doi:[10.1111/cns.14592](https://doi.org/10.1111/cns.14592)

SUPPORTING INFORMATION

Additional supporting information can be found online in the Supporting Information section at the end of this article.